Integration of Domestic Ventilation Systems with Vertical Axis Wind Turbine Ventilation Technology

Jirayut Sitthipuk
School of Engineering and Built Environment, Edinburgh Napier University, 10 Colinton Rd, Edinburgh, Scotland, EH10 5DT, UK

ABSTRACT

The use of natural ventilation components as an enhancement for the ventilation systems has become more desirable in the building sector. The natural ventilation systems play a crucial role in reducing the carbon footprint from space heating and cooling through applications of low carbon technology and heat recovery unit. Low carbon technologies such as windcatchers and turbine ventilators are commonly used in commercial, educational, and industrial buildings for providing thermal comfort within a building and minimising carbon emissions. This study proposes to investigate a new concept of home ventilation systems integrated with a vertical axis wind turbine. The study aims to achieve a more detailed understanding of the proposed system in terms of ventilation performance for both air extraction and supply of air by a turbine ventilator type. The simulation results of the proposed design of a turbine ventilator to meet the Building Regulation's minimum ventilation rate requirement are presented. Having considered a wind speed at 6 m/s, the maximum exhaust flow rate induced by the turbine ventilator was captured at 87.52 l/s, whereas the maximum air supply flow rate of 38.25 l/s induced by the air intake vent (AIV) was observed. To improve performance of the AIV, the simulation results of two modified versions (AIV1 and AIV2) show an increase in supply ventilation rate of 5% and 20% for the AIV1 and AIV2 respectively. As the proposed turbine ventilator is a primarily design, the results from this study indicate a promising potential of the ventilation system combined with a powerless turbine ventilator for domestic dwellings.

KEYWORDS

Turbine ventilator, ventilation

1 INTRODUCTION

The UK and EU are committed to reduce greenhouse gas emissions by at least 80% in 2050 compared to emission levels in 1990 transitioning to a low-carbon economy. HAVC (heating, ventilation and air-conditioning) system is a part of domestic buildings that is to warm up and cool internal occupied spaces, which provides acceptable indoor air quality (IAQ) and a comfortable environment in buildings through ventilation. In domestic dwellings, though air infiltration and natural ventilation are the primary ventilation method, it is considered less efficient in terms of energy savings for the building (Rhodes, 1995). Energy consumption of HVAC systems in building services accounts for 50% to 60% of the total energy consumption (Dimitroulopoulou, 2012; Ahmad et al., 2016). On the other hand, mechanical ventilators play a crucial role in a ventilation system where it can controllably provide consistent ventilation. With application of heat recovery, mechanical ventilation can have a significant impact on reducing energy consumption in buildings (Dodoo et al., 2011). However, they found that mechanical ventilation with heat recovery (VHR) system reduced the energy consumption for space heating and also increased the electrical energy consumption for its operation.

The reduction in energy consumption for heating and cooling is one of the global challenges as to achieving goals for decarbonisation in the building sector. As a part of the European Strategic Technology plan, the need of low carbon technologies for heating and cooling from

renewable energy sources has been highlighted in the past years. Applications of low carbon ventilation technologies e.g. powerless ventilators pose a prominent solution for reducing energy consumption in buildings (Tan et al., 2016). Powerless ventilators hold a potential to facilitate ventilation, reduce energy consumption and improve IAQ through the use of a renewable energy source - wind (Lai, 2003; Khan et al., 2008a; Tan et al., 2016).
With application of low carbon ventilation technology, a reduction in of energy demand with efficient supply can be achieved by using renewable energy resources. The drive of this research is to pursue a path of the nearly zero-energy building (NZEB) programme by the European Commission as a contribution for decarbonisation of heating and cooling in domestic dwellings.

This study is hypothesised to develop a new concept of home ventilation system by employing a wind driven turbine ventilator, as a means to reduce energy consumption and improve indoor air quality in a building. The proposed concept is to employ the new design of a turbine ventilator through modification based on a commercial wind-driven ventilator. This new turbine ventilator is designed to be capable to facilitate ventilation for both supplying fresh air and exhausting stale air. Thus, this study aims to achieve a more detailed understanding of the proposed system in terms of ventilation performance for both air extraction and supply of air by the turbine ventilator.

2 LITURATURE REVIEW

The influence of ventilation systems can affect heating and cooling loads in domestic dwellings, which results in energy consumption and greenhouse gas emissions (Guillén-Lambea et al., 2016). Heating and cooling loads are one of the primary sources that has an impact on residential energy consumption. As reviewed by Pérez-Lombard et al. (2008), the energy consumption of heating, ventilation and air-conditioning (HVAC) servicing in UK residential buildings accounts for 62% of the total energy consumption. Moreover, HVAC systems in building services can consume 50% to 60% of total end use energy (Ahmad et al., 2016). Therefore, the role of energy efficiency improvements is essential as a means to indicate the minimisation of energy consumption in buildings by implementing more energy efficient technologies and government policies (Peter G. Taylor et al., 2010). Ventilation technologies play a crucial part in energy efficiency improvements regarding energy concerns. Ventilation systems: natural or mechanical supply/exhaust types have significant impacts to improve IAQ and minimise energy consumption in domestic dwellings. However, optimisation of the ventilation systems usually depends on climate zones, heating & cooling demands and air quality requirement (Santos and Leal, 2012; Hesaraki et al., 2015; Guyot et al., 2018; Delwati et al., 2018; Zemitis and Borodinecs, 2019).

The use of natural ventilation components as an enhancement for the ventilation systems has become more desirable in the building sector. Low carbon technologies such as windcatchers and turbine ventilators are commonly used in commercial, educational and industrial buildings for cooling and ventilation purposes (Khan et al., 2008a). Powerless rotating or turbine ventilators are a wind-driven air exhaust technology that facilitates ventilation in domestic and industrial buildings (Khan et al., 2008b). Turbine ventilators are widely used especially in warm countries as an exhaust ventilation system to ease the intensities of poor IAQ and cooling loads of buildings, which reduces the energy consumption (Lai, 2003; Tan et al., 2016). As the climate gets warmer, energy consumption for more cooling demands of buildings can be reduced by employing turbine ventilators. However, overventilation can be an issue when applying this technology; Streckienė et al. (2018) found that the amount of air in a building was exhausted 12 to 41% more than its requirement. Khan et al. (2008b) also pointed that the use of the technology can cause energy losses in mild climate countries where the conservation of heat energy is needed in winter. Although turbine ventilators are the energy efficient technology for buildings in warm countries, there is a lack of robust studies on application of turbine ventilators in a ventilation system for domestic buildings in mild climate zones.

Another natural ventilation technology is windcatchers commonly used in education and industrial buildings to facilitate ventilation by wind and stack effect and to reduce cooling loads. In mild climates, a natural ventilation with heat recovery system can be achieved with windcatchers by employing a heat exchanger (Saadatian et al., 2012). An example of the windcatcher with heat recovery system is the Monodraught's Windcatcher HX with its capability of delivering cooling ventilation and heat recovery (Monodraught, 2020). However, when retrofitting conventional residential buildings, windcatchers have not been commonplace (Khan et al., 2008a; Jomehzadeh et al., 2020).

Decarbonising heating and cooling has become a hot topic in regard with the reduction in greenhouse gas emissions. Mechanical ventilation system usually consumes electricity for its operation (Russell et al., 2007; Lai et al., 2018; Delwati et al., 2018). Replacements for a more renewable and energy efficient technology are highly desired. This leads to the fundamental technique through the use of natural forces. Turbine ventilators hold a potential not only for ventilation in buildings, however, there is a lack of research on employing turbine ventilators in a balanced (supply & exhaust) ventilation system.

3 METHODOLOGY

3.1 CFD modelling

CFD analysis was conducted to explore flow patterns and performance of new design of a turbine ventilator. Numerical simulations were performed using SimScale and Autodesk CFD. The geometry of the turbine rotor domain is shown in Figure 1, where the diameter of the turbine, D is 400mm and the duct size, d is 140mm. The study of Alom and Saha (2019) showed that an elliptical blade profile exhibited better rotor performance than other blade profiles; semi-circular, Benesh and modified Bach rotors by 20.25%, 19.49% and 17.28% respectively. The elliptical blade profile was adopted with the blade height of 300mm, and the exhaust duct was extended 75mm from the rotor base. Furthermore, the air intake vent was designed to be 250mm high with a 35mm gap between louvers, which acts as a windcatcher, allowing fresh air flowing into building. A circular air intake vent was modelled with four openings (See Figure 1c).

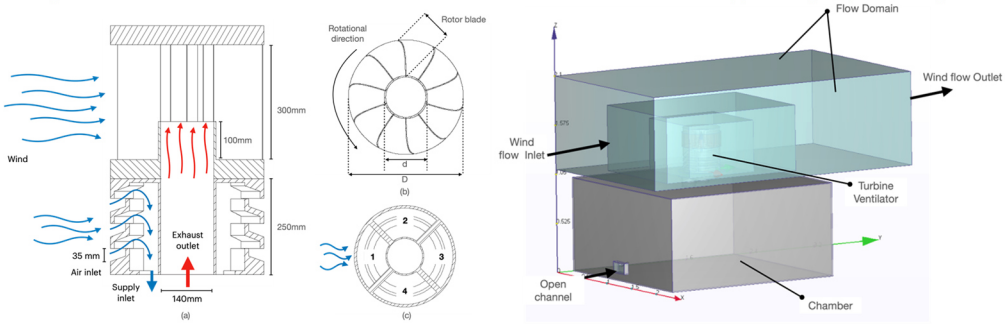

Figure 1. Schematic: (a) principle of the proposed turbine ventilator, (b) the geometrical parameters of the rotor domain, (c) air intake vent and (d) CFD computational domain setup.

3.2 Turbulence modelling, boundary conditions and grid details

The k-epsilon model, one of the most widely used turbulence models, is a robust model that is proficient in economically simulating a wide range of mean flow characteristics for turbulent flow conditions with reasonable accuracy. The standard k-epsilon turbulence model based on RANS was adopted in practical applications of many studies due to its good convergence and relatively low computation cost, which provides a reasonable estimate of complex flows through and around the turbine ventilator (Lien and Ahmed, 2010; Jadhav et al., 2016; Lan et al., 2021).

The present study adopted an CFD simulation approach of the wind tunnel domain setup for numerical simulations by Jadhav et al. (2016). The approach is a replication of the physical test rig for a wind tunnel. The whole computational domain consists of two primary regions: the

flow domain and the chamber (see Figure 1d). The overall size of the computational domain is 3D for the upstream x 5D for downstream extending to a width of 2.5D for both the right and left side boundaries and a height of 2.5D, where D is the diameter of the turbine ventilator.

Boundary conditions were assigned to each face of the computational domain. The entry of the computational domain upstream was defined as a uniform velocity-inlet boundary condition. The inflow rates were set to a variety of velocity magnitudes of 1, 2, 3, 4, 5 and 6 m/s, which was applied in the simulation. The rotation of turbine ventilators started when the wind speed was higher than 2 m/s (Rimdžius et al., 2018; Chen et al., 2019). A pressure outlet boundary condition was assigned to the end of the domain downstream of the turbine ventilator, in which the pressure was set equal to 0.

Due to the complexity of the geometry, tetrahedral meshing was employed to capture the flow characteristics in proximity of the geometry of interest, and to ensure the cell skewness was less than 1 and close to 0. The maximum skewness of the mesh was targeted to be equal to or less than 0.85 for a high-quality mesh (Lien and Ahmed, 2010; Ghanegaonkar et al., 2018; SIMSCALE, 2020). The total cell count of the computational domain was 2.12 million. The global maximum cell size was 4mm.

4 RESULTS AND DISCUSSION

4.1 Performance investigation of the initial turbine ventilator model

Settings for the velocity inlet are velocity magnitudes of 1 m/s, 2 m/s, 3 m/s, 4 m/s, 5 m/s and 6 m/s in the CFD analysis. The initial investigation was carried out by performing CFD simulation of the proposed turbine ventilator model with two different blade profiles of 2 blades (2B-TV) and 10 blades (10B-TV). This allows to quantify the influence of the turbine blade profile on the ventilation performance in terms of exhaust volume flow rate. CFD simulation of the 2B-TV with a throat diameter of 140mm was analysed. Figure 3a shows the velocity contours of the 2B-TV at different velocities. The contours of velocity were captured at 100 mm above the cylindrical base of the rotor domain. Having observed the flow pattern, a small region of recirculating flows appeared on the convex side of the blade at the top region facing the incoming flow direction. High velocity contours were captured at the convex side of the duct on the downstream. These highlighted zones have the influence on pressure distributions (see Figure 4). High pressure distribution can be recognised where the recirculation is formed. On the other hand, low pressure distribution is distributed on the duct subjected to high velocity contours.

In Figure 4, the correlations between high velocity and low pressure or low velocity and high pressure were captured and observed at 100 mm (a & b) and 160 mm (c & d) above the rotor base. The flow behaviour around the turbine ventilator is illustrated in Figure 4a, which indicates the recirculation zone of the incoming flow on the convex side of the returning blade (in the red circle) defecting the rotation of the turbine ventilator. This means the highlighted region is stagnant and creates a large pressure gradient on the blade convex (Tian et al., 2019). As a result, the flow separation was formed around the edge of the blade with a low-pressure region associated to a relatively high velocity. As the flow separation takes place, the flow behaviour in the middle region of the rotor indicates the swirling pattern of the flow as shown in Figure 4c. The swirling flows were produced near the inner edge of the returning blade. This allows the airflow to be removed and exhausted by the turbine ventilator from the duct. In Figure 4c, the upward arrows of the swirling flow represent the exhausted air being extracted. To further observe, the region where the swirling pattern produced has the influence on generating negative pressure as shown in Figure 4d. As a result, the more negative the pressure the better performance of air extraction is for the turbine ventilator.

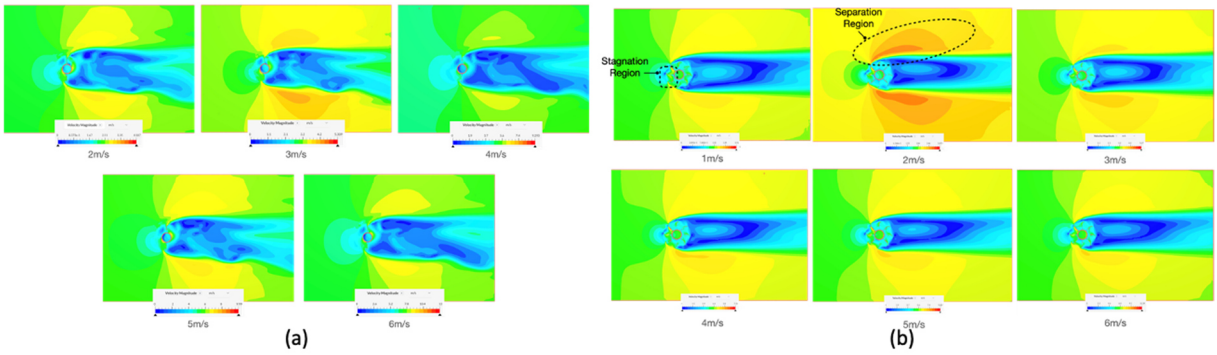

Figure 3. Velocity contours of the 2B-TV (a) and 10B-TV (b) at different velocities.

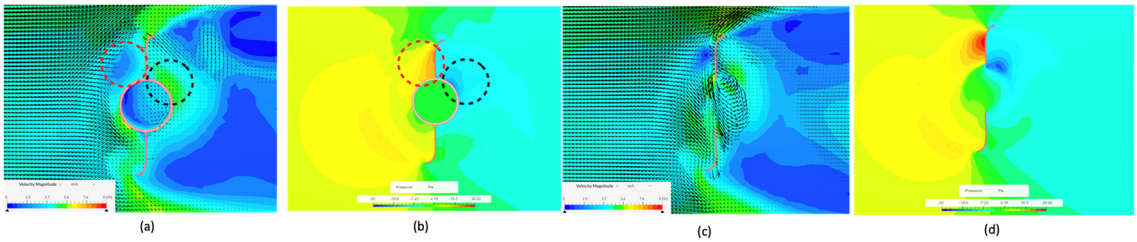

Figure 4. Velocity and pressure contours at velocity of 4 m/s.

For the 10B-TV model, CFD simulations were performed with a range of velocities between 1 m/s and 6 m/s. When the incoming flow interacts with the rotating blades, the stagnation region is formed which leads to the reduction in wind velocity of the rotating blade as shown in Figure 3b. Furthermore, the development of the separated flow is located at the top of the turbine ventilator, creating low pressure area. The incoming flows started entering the inner domain of the turbine ventilator from the top left corner and leaving through the bottom, causing the inner flows swirling in the interior of the turbine ventilator (see Figure 5). This behaviour of inner flows becomes the factor as the force contributing to the turbine rotation (Tian et al., 2019). It is observed that the interaction of the inner flows within the rotor caused a vortex to exist at the top right above the duct as shown in Figure 5b, which leads to the reduction in pressure around its area. The effect of stagnation region (in black circle in Figure 5a) caused the large positive pressure occurred on the tip of the returning blade zone (in red circle in Figure 5c). With an increase in wind speed of the inner flow coming through the rotor, it is observed that the development of negative pressure was influenced by the inner flow velocity as shown in Figure 5d. It indicates that the 10-blade profile had a great impact on the pattern of swirling flows to induce greater extraction flow rates.

The performance of the AIV was assessed against an induced flow rate entering through the AIV model. The CFD simulation was performed under a steady state condition and with an angle of the wind flow inlet at 0°. The CFD result of the AIV model at a velocity magnitude of 6 m/s is exhibited. Figure 6a shows the distribution of velocity field at the bottom of the AIV supply channels, where the induced flow passes through the opening on the windward side of the channel. The vector of velocity indicates the flow patterns of the oncoming wind from the windward side captured and induced by the AIV, while the airflow can be seen leaving at other channels (see Figure 6b).

In Figure 6c, it is notable in the velocity contours that the recirculation zones were formed on outer wall at lower edge of the louver bend (in red circle) after the airflow entered the inlet opening. This flow separation is caused by a sudden change in the flow direction at sharp corners at the bend, which leads to a negative impact on the performance of the supply airflow rate (Alsailani et al., 2021). As the flow keeps moving towards the rear wall, it accelerated the formation of a larger recirculation zone and flow separation to take place.

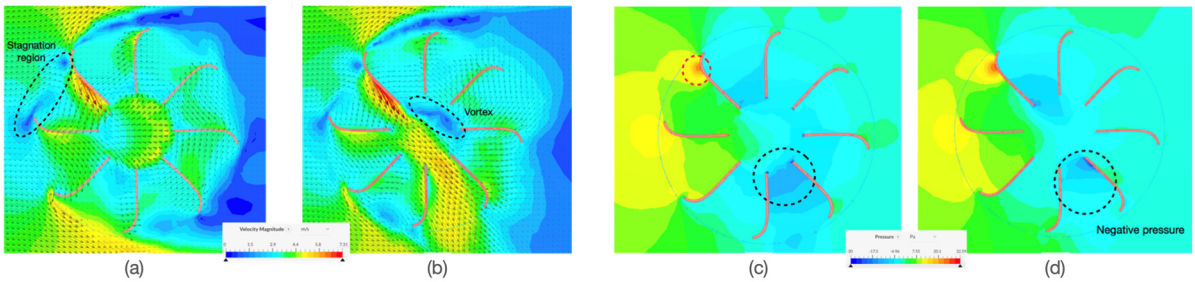

Figure 5. Velocity and pressure contours at 4 m/s of the 10B-TV at 300 mm above the cylindrical base.

The pressure contours of the cross-sectional plane of the supply channel indicate a large pressure gradient produced near the upper wall of the bend, as well as at the louver (See Figure 6d). This indicates that the high-pressure area has a negative impact on the loss in the air flow, which leads to a decrease in mass flow rate in the air supply channel. Having performed CFD simulation at a velocity of 6 m/s, the result of the average pressure of the AIV supply channel was captured at 27.26 Pa, while the AIV induced the air supply rate of 38.25 l/s. Given the numerical results of its ventilation performance, there are still rooms for improvements in terms of minimising in flow losses through modifications of features of the AIV.

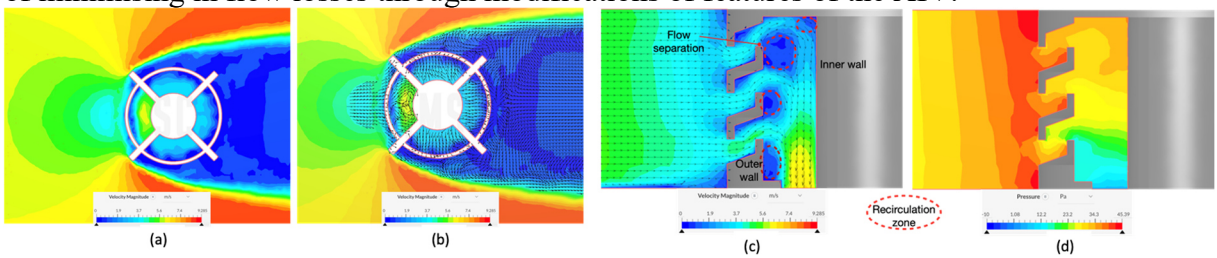

Figure 6. AIV velocity contour and cross-sectional plane: (c) velocity and (d) pressure contour.

The comparison of the numerical results of the ventilation performance between the 2B-TV and 10B-TV models. The results of exhaust mass flow rates were plotted against wind speed (See Figure 7a). It is noticeable that the 10B-TV greatly outperformed the 2B-TV by 66% after the wind speed above 2 m/s. Given the velocity speed at 6 m/s, the exhaust mass flow rate extracted by the 2B-TV did not meet the benchmark of the ventilation rate of 35 l/s for dwellings. On the contrary, the 10B-TV managed to satisfy the minimum ventilation rate at the velocity speed of 3 m/s with the extracted volume flow rate of 35.59 l/s. By comparing the ventilation performance between the two models, it is evident that the 10B-TV model demonstrates the better performance for exhaust ventilation flow rates.

To validate the CFD results of ventilation performance of the 10B-TV model in this study, the results were further compared with the experimental and numerical results produced by (Khan et al., 2008b; Ghanegaonkar et al., 2018). The results of 300 mm and 250 mm straight vane turbine ventilators obtained from the experiment of Khan et al. (2008b) and a 600 mm curved turbine ventilator by Ghanegaonkar et al. (2018) were considered for the comparison against the CFD results of the present study. In Figure 7b, it is observed that the results of the present study were found to be in agreement with the results of a 250 mm straight vane turbine ventilator by Khan et al. (2008b).Though there is difference in size of the throat diameter, the 10B-TV with a throat diameter of 140 mm is capable to induce air flow as much as the 200mm turbine ventilator. Nevertheless, the overall trend in ventilation performance of the 10B-TV was shown to be in good agreement with the results of other studies.

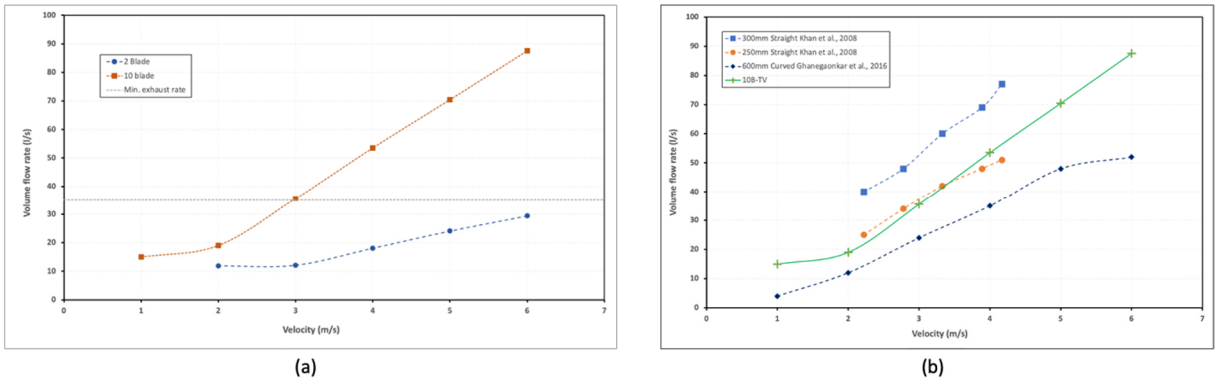

Figure 7. Comparison of the ventilation performance: (a) 2B-TV and 10B-TV and (b) with other studies.

The simulation results of the volume flow rates induced by the AIV model were plotted against a range of velocity from 2 m/s to 6 m/s as shown in Figure 9a. It indicates that a linear relationship of the increasing induced flow rates is influenced by increases in wind velocities. With the suggested ventilation rate, he induced flow rates of the AIV meet the minimum requirement for 1, 2, 3 and 4 bedrooms when the wind speed remains at 3.8 m/s, 5 m/s, 5.5 m/s and 6 m/s respectively.

4.2 Performance investigation of modified turbine ventilator model

With 50% increasing the height of blades, the mass flow rates can be improved by 13.5% (Khan et al., 2008b). A decrease in blade height was considered in this study to determine the differences in performance of the turbine blades to be more efficient at a lower wind speed. In Figure 8, it demonstrates the formation of vortices taking place in the mid region of the rotor with respect to an increasing wind speed. With interactions of the incoming flow on the windward side of the modified 10B-TV, a stagnation point was formed, where the local velocity is equivalent to zero. Consequently, the large positive pressure was produced on the convex side of the returning blades (see Figure 8b). This stagnation point flow extended towards the upper along the rotating blades. With deacceleration from the stagnation point flow, a flow separation was taken in place upstream of the rotor domain. The distribution of pressure was determined by the flow velocity, where the large positive pressure was formed in the low velocity area. Inversely, the low-pressure area was taken place at the high velocity region. Hence, the exhaust flow rate of 45.18 l/s at a 6 m/s wind speed was obtained. The exhaust flow rates obtained from the CFD simulations were plotted against with respect to different velocities (see Figure 9b). It is observed that the performance of the modified 10B-TV was better than the 2B-TV by between 32% and 45% after passing 3 m/s, while it underperformed with almost 50% difference comparing to the 10B-TV.

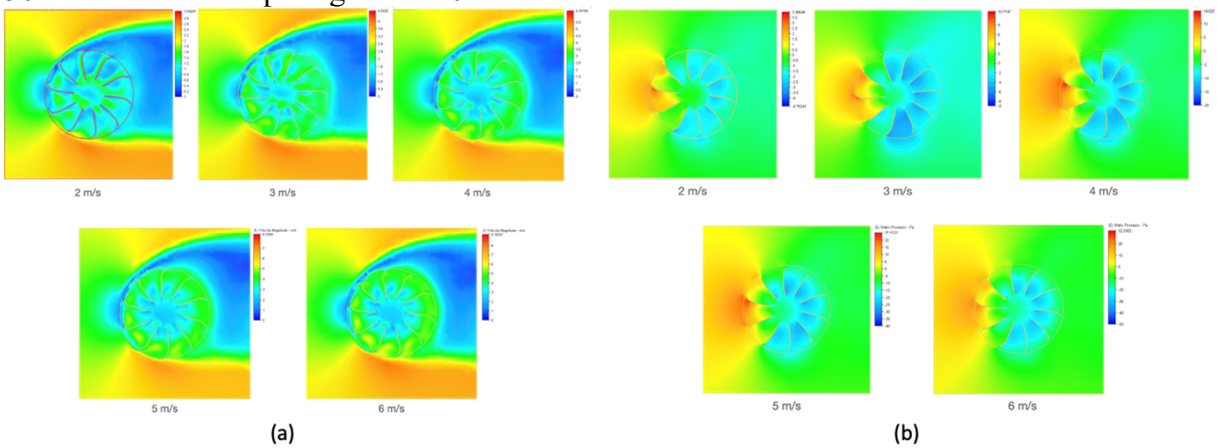

Figure 8. The modified 10B-TV: (a) velocity contour and (b) pressure contour.

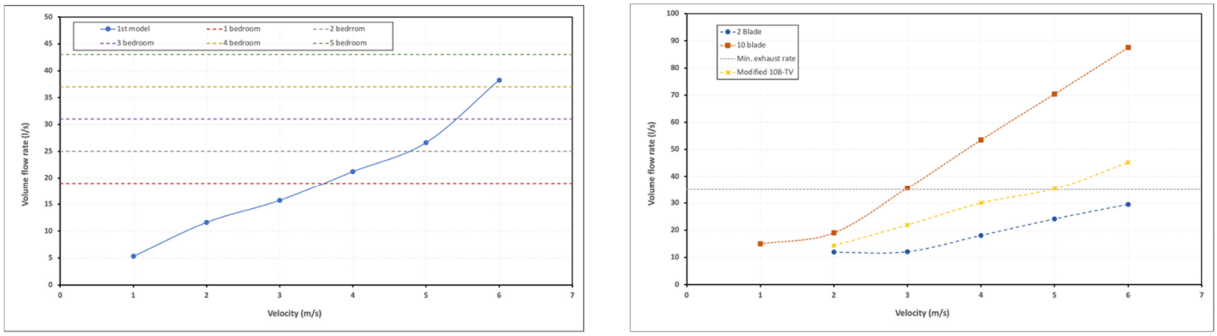

Figure 9. (a) Volume flow rates induced by the AIV model and (b) Comparison of ventilation performance.

Furthermore, the development of recirculation zones of the AIV is due to separated flow formed near corners at the bend. This leads to an increase in flow losses, resulting in a pressure drop. To reduce a drop of pressure in the AIV, altering features of the AIV profile was considered. Since flow separation and recirculation zones occur at sharp corners of the bend, the 90° bends of the louvers at inlet opening were simplified as the AIV1 model (see Figure 10). Alsailani et al. (2021) found that adding guide vanes in the bends could substantially improve the uniformity of air flow within the supply channel, which led to an increase in airflow rate up to 29%. Hence, the modified AIV2 model was modified by rounding sharp corners at the bend and adding guide vanes at the end of the inlet opening. The CFD results of the modified AIV1 and AIV2 at a velocity of 6 m/s are presented. Figure 10a shows that the size of recirculation zones (in the red circle) was reduced when compared to the large recirculation zones of the AIV in Figure 6c. This allows an increase in air flow to travel inside the supply channel, which reduces pressure drop in the supply channel as shown in Figure 10b. The supply flow rate of air supply induced by the modified AIV1 was determined at 40.83 l/s with respect to a wind speed of 6 m/s.

Moreover, in Figure 10c. It is observed that the formation of recirculation zones compared to the AIV was not reduced as much as expected. Noticeably, the air flow increased due to the influence of the rounded corner and guide vane directing the flow at the separation point to travel the same way. The maximum velocity of 8.37 m/s was measured in the channel and considered higher compared to the modified AIV1 with the maximum velocity of 6.81 m/s. Hence, it results that the pressure drop was significantly reduced with the design of the modified AIV2 as shown in Figure 10d. It is clear that the corelation between air flow and pressure, when pressure decreases, reversely air flow increases. The volume of supply air flow rate was gauged at 48.11 l/s. With the influence of these modified AIV1 and AIV2, the ventilation performance of the AIV can be improved by 5% for the modified AIV1 and 20% for the AIV2.

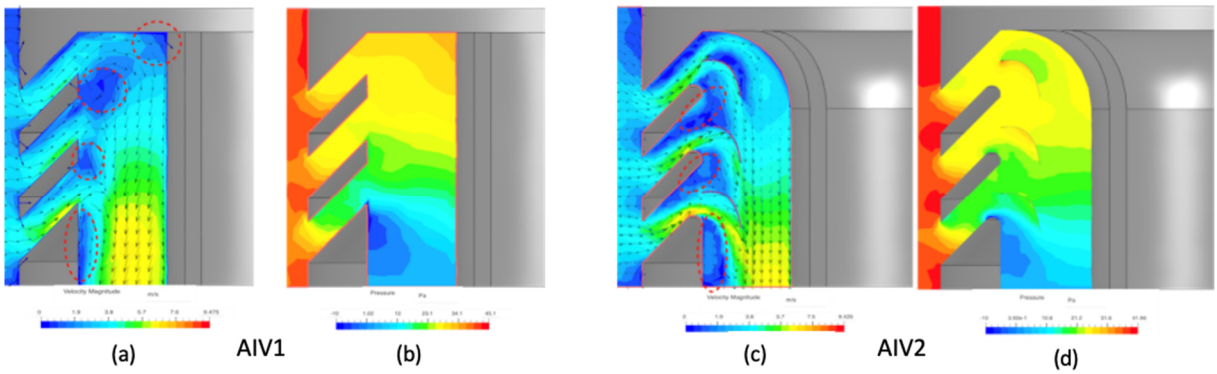

Figure 10. Velocity and pressure contours: (a) Modified AIV1 and (b) Modified AIV2.

5 CONCLUSIONS

The present study was conducted to initially investigate a new concept of home ventilation system integrated with turbine ventilator, as a means to reduce its energy consumption and improve indoor air quality in a building. A model of a turbine ventilator was designed to be capable of both supplying fresh air in and exhausting stale air from a building. The primary focus of the study was to explore the ventilation performance of the proposed turbine ventilator. CFD simulations were carried out using SimScale and Autodesk CFD to predict the ventilation performance of the proposed turbine ventilator.

CFD simulations were first carried out to explore the influence of blade profile by testing a 2 blade (2B-TV) and a 10 blade (10B-TV) models. For air extraction, the numerical results show that the 10B-TV outperformed the 2B-TV by 66% at velocity speed 3 m/s and above. The maximum exhaust flow rate induced by the 10B-TV was captured 87.52 l/s at a wind speed of 6 m/, which exceeded the minimum ventilation rate. Although a modification of the 10B-TV was made, there were no improvements for ventilation performance. Validation of the CFD results was conducted by a comparison with experimental results from other studies. It indicated the results of the present study were found to be in agreement with the results of a 250 mm straight vane turbine ventilator by Khan et al. (2008b). The initial design of the air intake vent (AIV) was tested, which result in the maximum flow rate of air supply of 38.25 l/s at 6 m/s. However, the AIV did not meet the minimum ventilation rate. The AIV was modified in order to improve it ventilation performance. As a result, the modified AIV1 and AIV2 induced a higher supply flow rate than the original AIV by 5% and 20% respectively. With the results of the AIV2, the minimum requirement for 5 bedroom was satisfied.

As the proposed turbine ventilator is a primary design, the study shows a promising potential of the proposed home ventilation system integrated with the turbine ventilator. With further improvements, this new concept of ventilation system could be a greener alternative for future home ventilation for new builds or conventional houses. The application of powerless turbine ventilator to induce exhaust air flow rate through the roof is effective and efficient for the industrial buildings. However, it is deemed as unnecessary for domestic ventilation systems, mainly due to required working environment, visual pollution for some homeowners and unreliable resource for operation. It is being underrated in a ventilation strategy as compared to HVAC, where it is considered more efficient in terms of both energy saving and ventilation. It will be cheaper and greener for domestic dwellings if a new ventilation system integrated with a low carbon turbine ventilator that maximises a natural source of wind energy for ventilation and energy saving can be developed.

6 REFERENCES

Ahmad MI, Mansur FZ and Riffat S (2016) Applications of Air-to-Air Energy Recovery in Various Climatic Conditions: Towards Reducing Energy Consumption in Buildings. Renewable Energy and Sustainable Technologies for Building and Environmental Applications. pp.107-116.

Alom N and Saha UK (2019) Influence of blade profiles on Savonius rotor performance: Numerical simulation and experimental validation. Energy Conversion and Management 186: 267-277.

Alsailani M, Montazeri H and Rezaeiha A (2021) Towards optimal aerodynamic design of wind catchers: Impact of geometrical characteristics. Renewable Energy 168: 1344-1363.

Chen T, Huang C and Kuo Y (2019) Numerical Study on Air Extraction Performance of Rooftop Ventilators. Journal of Aeronautics, Astronautics and Aviation 51: 075 - 086.

Delwati M, Merema B, Breesch H, et al. (2018) Impact of demand-controlled ventilation on system performance and energy use. Energy and Buildings 174: 111-123.

Dimitroulopoulou C (2012) Ventilation in European dwellings: A review. Building and Environment 47: 109-125.

Dodoo A, Gustavsson L and Sathre R (2011) Primary energy implications of ventilation heat recovery in residential buildings. Energy and Buildings 43(7): 1566-1572.

Ghanegaonkar PM, Jadhav GK and Garg S (2018) Performance improvement of turbo ventilators with internal blades. Advances in Building Energy Research 12(2): 164-177.

Guillén-Lambea S, Rodríguez-Soria B and Marín JM (2016) Review of European ventilation strategies to meet the cooling and heating demands of nearly zero energy buildings (nZEB)/Passivhaus. Comparison with the USA. Renewable and Sustainable Energy Reviews 62: 561-574.

Guyot G, Sherman MH and Walker IS (2018) Smart ventilation energy and indoor air quality performance in residential buildings: A review. Energy and Buildings 165: 416-430.

Hesaraki A, Myhren JA and Holmberg S (2015) Influence of different ventilation levels on indoor air quality and energy savings: A case study of a single-family house. Sustainable Cities and Society 19: 165-172.

Jadhav GK, Ghanegaonkar PM and Garg S (2016) Experimental and CFD analysis of turbo ventilator. Journal of Building Engineering 6: 196-202.

Jomehzadeh F, Hussen HM, Calautit JK, et al. (2020) Natural ventilation by windcatcher (Badgir): A review on the impacts of geometry, microclimate and macroclimate. Energy and Buildings 226.

Khan N, Su Y and Riffat SB (2008a) A review on wind driven ventilation techniques. Energy and Buildings 40(8): 1586-1604.

Khan N, Su Y, Riffat SB, et al. (2008b) Performance testing and comparison of turbine ventilators. Renewable Energy 33(11): 2441-2447.

Lai C-m (2003) Experiments on the ventilation efficiency of turbine ventilators used for building and factory ventilation. Energy and Buildings 35(9): 927-932.

Lai C-M (2006) Prototype development of the rooftop turbine ventilator powered by hybrid wind and photovoltaic energy. Energy and Buildings 38(3): 174-180.

Lai D, Qi Y, Liu J, et al. (2018) Ventilation behavior in residential buildings with mechanical ventilation systems across different climate zones in China. Building and Environment 143: 679-690.

Lien S-TJ and Ahmed NA (2010) Numerical simulation of rooftop ventilator flow. Building and Environment 45(8): 1808-1815.

Lien STJ and Ahmed NA (2011) Effect of inclined roof on the airflow associated with a wind driven turbine ventilator. Energy and Buildings 43(2-3): 358-365.

Monodraught (2020) Natural ventilation product brochure. Available at: https://www.monodraught.com (accessed 2 June).

Pérez-Lombard L, Ortiz J and Pout C (2008) A review on buildings energy consumption information. Energy and Buildings 40(3): 394-398.

Peter G. Taylor, Olivier Lavagne d'Ortigue, Michel Francoeur, et al. (2010) Final energy use in IEA countries: The role of energy efficiency. Energy Policy 38(11): 6463-6474.

Rhodes N (1995) Heating, ventilating and air conditioning analysis and design. Proceedings of the Institution of Mechanical Engineers 209(2): 163.

Rimdžius D, Bielskus J, Martinaitis V, et al. (2018) Experimental Evaluation of Turbine Ventilators Performance under Different Test Conditions. E3S Web of Conferences 64.

Russell M, Sherman M and Rudd A (2007) Review of Residential Ventilation Technologies. HVAC&R Research 13(2): 325-348.

Saadatian O, Haw LC, Sopian K, et al. (2012) Review of windcatcher technologies. Renewable and Sustainable Energy Reviews 16(3): 1477-1495.

Santos HRR and Leal VMS (2012) Energy vs. ventilation rate in buildings: A comprehensive scenario-based assessment in the European context. Energy and Buildings 54: 111-121.

SIMSCALE (2020) SimScale Documentation. Available at: https://www.simscale.com/docs/ (accessed 11 June).

Streckienė G, Motuzienė V, Rimdžius D, et al. (2018) Simulation of Annual Functionality of Roof Turbine Ventilator. E3S Web of Conferences 64.

Tan YC, Ismail M and Ahmad MI (2016) Turbine Ventilator as Low Carbon Technology. Renewable Energy and Sustainable Technologies for Building and Environmental Applications. pp.167-174.

Tian W, Mao Z and Ding H (2019) Numerical study of a passive-pitch shield for the efficiency improvement of vertical axis wind turbines. Energy Conversion and Management 183: 732-745.

Zemitis J and Borodinecs A (2019) Energy saving potential of ventilation systems with exhaust air heat recovery. IOP Conference Series: Materials Science and Engineering 660: 012019.